

# Highly Sensitive and Selective Fluorescent Sensor for Ag<sup>+</sup> in Using $\beta$ -Cyclodextrin / Chitosan Polymer Coated S QDs Based on Aggregation Caused Quenching Mechanism

Shan Wang (✉ [shanwang2002@163.com](mailto:shanwang2002@163.com))

Xianyang Normal University

Huan Wang

Xianyang Normal University

Jianshe Yue

Xianyang Normal University

Yi Lu

Xianyang Normal University

Tian Jia

Xianyang Normal University

Jie Chen

Xianyang Normal University

---

## Research Article

**Keywords:** S QDs, CTSCD nanocomposites, Silver ions, Fluorescent, Sensor

**Posted Date:** February 12th, 2021

**DOI:** <https://doi.org/10.21203/rs.3.rs-184383/v1>

**License:**   This work is licensed under a Creative Commons Attribution 4.0 International License.

[Read Full License](#)

---

# Abstract

A fluorometric sensor based on poly ( $\beta$ - cyclodextrin/chitosan) with H bonded S QDs/CTSCD nanocomposites was synthesized by self-assembly. They were characterized by FTIR, UV-Vis spectroscopy, XPS, and TEM. The S QDs on the chain of the polymer could coordinate with transition-metal ions due to surface electronegativity. The distance between the S QDs on the different chains of polymer could construct the bridge bond of S-Ag<sup>+</sup>-S with silver ions leading to fluorescence aggregation-caused quenching. The linear range of the method was from  $1.0 \times 10^{-5}$  -  $5.5 \times 10^{-5}$  mol/L. The correlation coefficient was 0.9992 with a detection limit of 66.7 nM. This method could be used to detect silver ions in real samples with excellent sensitivity and selectivity, indicating its potential as a novel sensor.

## Highlights

Facile fabrication of a novel bionanomaterials to detect silver ions in water by aggregation-caused quenching mechanism

(1) A green coordination mechanism-based S QDs fluorescence sensor was easily fabricated.

(2) The S QDs/CTSCD nanocomposites could coordinate with Ag<sup>+</sup> due to surface electronegativity.

(3) The aggregation caused quenching mechanism of the sensor form the bridge bond of S-Ag<sup>+</sup>-S with Ag<sup>+</sup>.

## 1. Introduction

Silver ions were a precious metal with special bactericidal, catalytic, and optical properties [Velmurugan, 2014]. The metal was widely used in electronics, photo-sensing, and electroplating industries, causing silver ions to enter the environment in various forms. Silver ions were one of the most toxic metal ions for aquatic organisms even at 0.5% concentration [Singh, 2020; Nasrollahzadeh, 2021; Zhang, 2020]. At the same time, a large amount of silver-containing industrial waste was constantly released into the environment. The 17  $\mu\text{g/L}$  concentration of silver ions was also harmful to the fish and microorganisms. Thus, the detection silver ions had become an important topic of health, epidemic prevention, and environmental monitoring. There were many ways to detect heavy metal ions such as stripping voltammetry, [Mikelova, 2007] atomic absorption spectrometry, [Chamsaz, 2008] inductively coupled plasma mass spectrometry [Barriada, 2007] et al. But all of these were non-portable, expensive, time consuming [Lin, 2010;]. Therefore, the design of novel detection methods for selectivity and sensitivity to silver ions was crucial for the maintenance of the environment and human health. Fluorescence analysis, a highly sensitive and selective determination method had developed rapidly in recent years. Because this method could not only overcome the above shortcomings, but also solve the serious drawbacks such as low sensitivity, hydrophobicity, low selectivity, and toxicity, et al [Jaiswal, 2012; Zheng, 2013; Ding, 2010].

As long as the appropriate fluorescent substances were selected, fluorescence quenching for detecting trace silver ions could be established [Singha,2015]. A few fluorescent sensors for sulfur atoms have been reported for silver ions determination in recent years[Goh,2017;Hwang,2017; Lotfi,2017]. However, many of them had poor biocompatibility and poor water solubility, which hindered their application in water and biological environment. Therefore, the development of biocompatible and water-soluble fluorescent sensors for silver ions was one of the areas which scientists focus on. So far, a wide variety of fluorescent probes had been developed, including metal nanoparticles, semiconductor quantum dots and dye molecules to solve the disadvantages of low sensitivity, low selectivity, insoluble, toxic and so on[Gao,2015]. S QDs have good stability, low cytotoxicity and high biocompatibility. It was found that there were almost no fluorescent probe to detect silver ions by using S QDs in the literature [Fu,2020]. Therefore, it was necessary to develop high-sensitivity, green, portable, and low-cost S QDs fluorescence sensors to detect silver ion.

Several coordination mechanism-based sensors for detecting ions had been exploited [Luidmila,2017; Xiao,2010]. However, most of these coordination polymers were macroscopic solid-state substances, which had very limited solution-based behavior. Given the hydrophobic ligands of the prepared complex polymers, the sensing reaction was primarily performed in an organic solvent. This characteristic remarkably limited their application in biosensors. The polymers had a tailorable and diversified structure and provide a new possibility for their use as biosensors [Spokoyny, 2009; Lotfia,2017; Vaishnav,2019;Jiang,2018].

We proposed a new method to detect silver ions with high sensitivity and excellent selectivity. Chitosan (CS) and  $\beta$ -cyclodextrin was formed a novel polymer crosslinked by formaldehyde (CTSCD). The S quantum dots (QDs) were combined with the amino group in the CTSCD by an electrostatic effect to form the S QD/CTSCD nanocomposites. The S QD /CTSCD nanocomposites rapidly aggregated in the presence of silver ions because of its attraction to the surrounding of S QD/CTSCD nanocomposites through electrostatic interaction.  $S-Ag^+-S$  was formed with the S QD/CTSCD nanocomposites leading to remarkable particle aggregation and aggregation-caused quenching (ACQ) occurred during its fluorescence detection. The possible mechanism was shown in Figure 1.

## 2. Experimental

### 2.1 Reagents and instruments

All chemical reagents were bought from Aladdin Reagent (Shanghai) Co., Ltd and used without further purification. Secondary distilled water was used throughout the experiments. Fluorescence was recorded on a Fluoromax-F 7000 spectrofluorometer with a 10 nm slit and UV-vis spectra were determined using a Shimadzu UV-24500 equipment. XPS data were obtained with an Axisultra DLD electron spectrometer from Shimadzu. FTIR spectra were recorded on Nicolet Magna 550 spectrometer.

### 2.2 Preparation of CTSCD.

Exactly 3.00 g of CS was completely dissolved in 300 mL (0.1 mol/L) of hydrochloric acid, and 15.00 g of  $\beta$ -cyclodextrin was dissolved in 600 mL of distilled water. The above mentioned prepared solution was mixed in a 1000 mL beaker. The temperature was increased to 60°C, and 25.00% of the formaldehyde (14.40 mL) was added slowly. The temperature was then increased to 90°C, and the reaction was carried out at stirring for 80.00 mins. After the reaction was completed, NaOH was added dropwise to the solution until pH reached 11.00, and a yellow precipitate was produced. The same temperature was maintained, and the reaction was continued for 45 mins. The reaction solution was filtered, washed to neutral, and washed with acetone and ethanol twice. The extract was dried to a constant weight at 45°C. The resulting product was a CTSCD with a red-brown color.

### 2.3 S QDs functionalized CTSCD

Exactly 0.031 g of CTSCD was dissolved in 6.0 mL of anhydrous ethanol. Then, 1.50 mL (3 mg/mL) of S QDs was added to the solution. The tube was placed in an ultrasonic instrument to complete self-assembly synthesis, and the sample S QD/CTSCD nanocomposites were obtained.

### 2.4. Fluorescence properties of S QD/CTSCD nanocomposites

The fluorescence sensing silver ions in the sample by S QD/CTSCD nanocomposites was determined as follows: different concentrations of silver ions were mixed with 500  $\mu$ L of S QD/CTSCD nanocomposites and 2.5 mL ultrapure water. After 5 min, the solution was transferred to the luminous measurement with an excitation wavelength of 295 nm. The excitation wavelength ( $\lambda_{ex}$ ) of S QDs/CTSCD nanocomposites was 295 nm in all tests, and the emission was monitored from 320 nm to 580 nm. The width of excitation and emission slit was 5 nm.

The selectivity of silver ions was investigated by preparing the same samples following the above mentioned.  $Fe^{3+}$ ,  $Ca^{2+}$ ,  $Pb^{2+}$ ,  $Na^+$ ,  $Cr^{3+}$ ,  $Bi^{3+}$ ,  $Zn^{2+}$ ,  $Mg^{2+}$ ,  $Ba^{2+}$ ,  $Cd^{2+}$ ,  $Ag^+$ ,  $Sr^{2+}$ ,  $Hg^{2+}$ ,  $Ni^{2+}$ , and other solutions were added to each sample until the same concentration (10  $\mu$ M) was reached. All of the mixtures were incubated at room temperature for 20 mins. The fluorescence spectra were recorded at the excitation wavelength of 295 nm.

### 2.5 Application in actual water samples

The practicability of the method was evaluated by detecting the actual water samples from the iron bridge, Xianyang Lake, Canal water, and tap water. The impurities were removed by filtration and centrifugation, and silver ions in river samples was detected by standard addition method. The detection procedure was the same as the above mentioned.

## 3. Results And Discussion

### 3.1. FTIR and DSC analysis of the S QD/CTSCD nanocomposites

Fig.2A showed the infrared spectra of the S QDs, CTSCD, and S QD/CTSCD nanocomposites. The peak at  $1640\text{ cm}^{-1}$  was a typical S QDs [Shan,2019], and the peak at  $896\text{ cm}^{-1}$  was  $\beta$ -(1, 4)-glycosidic bonds of CS. The peak at  $1042\text{ cm}^{-1}$  indicated the presence of the  $\alpha$ -(1,4)-glycosidic bond of  $\beta$ -CD. The peak at  $1640\text{ cm}^{-1}$  corresponded to the S QDs, indicated that S QDs was successfully introduced to CTSCD. The peaks at  $1560\text{--}1640\text{ cm}^{-1}$  and  $2100\text{ cm}^{-1}$  were belonging to amino ( $-\text{NH}_2$ ), alicyclic amine I ( $\text{C}=\text{O}$ ), and cyclic amine II ( $\text{N}-\text{H}$ ) groups. The absorption peak of the S QD/CTSCD nanocomposite was reduced due to the reaction with the amino group.

The results of DSC analysis of CTSCD (a) and S QD/CTSCD nanocomposites (b) were shown in Fig. 2B. Curve a showed an obvious endothermic peak at  $97.25^\circ\text{C}$  attributed to the crystalline water that evaporated in the CTSCD. The melting peak of CS was approximately  $225^\circ\text{C}$  due to the internal H bond, whereas the melting peak of CTSCD was approximately  $228^\circ\text{C}$ , which was more stable than that of the CS monomer [Djerahov,2016Teng, 2020. Rao, 2020, Lin,2020, Li, 2020]. From the curve b in Fig.2B, an obvious endothermic peak was found at  $100^\circ\text{C}$ . The hydrophobicity and thermal stability of CTSCD were evidently improved by the S QDs. The exothermic peak at  $259.48^\circ\text{C}$  was the degradation peak of S QD/CTSCD nanocomposite chain skeleton, which was due to the weakening of hydrogen bond interaction and the destruction of crystal structure regulation by S QDs. The two lines in Fig.2B showed that with increased degradation temperature of the chain skeleton, the thermal stability of S QD/CTSCD nanocomposites were improved.

### 3.2. Optical property and TEM of the S QD/CTSCD nanocomposites

The optical properties of S QDs/CTSCD were studied on the basis of the UV absorption spectra and fluorescence spectra at room temperature. Fig.3A showed a  $298\text{ nm}$  centered absorbance band in the UV absorption spectrum. The ultraviolet absorption of S QDs, which was modified by the CTSCD polymer, was stronger than that of S QDs. Therefore, as shown in Fig.3A, the solution of S QD/CTSCD nanocomposites was light yellow (A) in sunlight but bright blue when irradiated at  $365\text{nm}$  UV light (B), indicating the blue fluorescence properties of S QD/CTSCD nanocomposites. When excited at  $295\text{ nm}$ , the fluorescence spectrum showed excellent emission peak at approximately  $411\text{ nm}$ , which was shown in Fig.3B.

The TEM micrographs (Fig. 4A) showed the good dispersion of S QDs. The particles mostly have a regular spherical shape with approximately  $2\text{--}3\text{ nm}$  in size. A typical amorphous structure was observed with no visible lattice. These results showed that the synthetic S QDs had excellent nanoparticle properties for metal-ion sensors. The atomic force microscopy image shows the shape and height of the S QDs. The average height was  $2.8\text{ nm}$  (Fig. 4B). The TEM image showed the good dispersion of SQD/CTSCD (Figs.4B and 4C) with a relatively uniform size distribution. The average diameter of the S QDs/CTSCD was  $2.5\text{ nm}$ .

### 3.3. XPS of S QD/CTSCD nanocomposites

The composition, surface group, and structure of S QDs/CTSCD were studied by XPS. The four peaks of the nanocomposites at 284.30, 398.8, 532.04, and 165.9 eV were C1s, N1s, O1s, and S2p in the Fig.5A, respectively. The C1s spectrum (Fig.5B) had two peaks at 282.73 and 285.9 eV, which could be attributed to C–C and C–OH. Two peaks were found at 165.75 and 165.5eV in the S 2p spectra (Fig. 5C) attributed to S in  $\text{SO}_2^-(2p^{2/3})$ ,  $\text{SO}_2^-(2p^{1/2})$ ,  $\text{SO}_3^-(2p^{2/3})$ , and  $\text{SO}_3^-(2p^{1/2})$  bands [Prasannan,2013]. The three peaks of 395.9, 396.05, and 397.1eV in the N1s spectrum (Fig.5D) were from the C–N–C and C–N groups, respectively. The O1s spectrum (Fig.5E) had two peaks at 532.7 and 531.9eV, which were due to the C–OH/C–O–C and C=O bands [Park,2015;Teng,2020;Wu,2020]. This finding indicated that S atom was added to the CTSCD prepared in the present study. These results were consistent with those of FTIR.

### 3.4 Effect of pH on the fluorescence of S QD/CTSCD nanocomposites

Fig.6 showed the effect of pH (4–10) on the fluorescence intensity of the S QD/CTSCD aqueous solution. In the experiments, 0.1 M HCl and NaOH were added to the solution to obtain the desired pH. In the strong acid environment( $\text{pH} \leq 4$ ), the amino groups on chitosan will protonate [Gao,2020;Yang,2020], which would destroys the weak self-assembly between the polymer and sulfur quantum dots. The sulfur quantum dots fall from the polymer chain, the fluorescence intensity increased significantly ( $\text{pH}=4$ ). With increased pH from 4 to 10, fluorescence intensity decreased by approximately 7%. This negligible change might be the result of a small change in the quantum confinement due to the functionalization of the S QDs/CTSCD. S QD/CTSCD samples did not change their maximum fluorescence value and the same spectral shape was changed. Under these experimental conditions, the S QD/CTSCD samples were monodispersed and the fluorescence emission was stable [Dager,2019].

### 3.5. Selectivity of the sensor

Selectivity was an important parameter for assessing the fluorescence property of S QD/CTSCD nanocomposites. The effect of various metal ions, such as  $\text{Fe}^{3+}$ ,  $\text{Ca}^{2+}$ ,  $\text{Pb}^{2+}$ ,  $\text{Na}^+$ ,  $\text{Cr}^{3+}$ ,  $\text{Bi}^{3+}$ ,  $\text{Zn}^{2+}$ ,  $\text{Mg}^{2+}$ ,  $\text{Ba}^{2+}$ ,  $\text{Cd}^{2+}$ ,  $\text{Ag}^+$ ,  $\text{Sr}^{2+}$ ,  $\text{Hg}^{2+}$ , and  $\text{Ni}^{2+}$  which concentration was  $1.0 \times 10^{-5} \text{ mol/L}$  of fluorescence was examined. As shown in Figure 7 (A), the fluorescence intensity of S QD/CTSCD nanocomposites was quenched to a remarkable extent in the presence of silver ions, whereas the fluorescence intensity in other metal ions (alkali, alkali soil, and transition-metal ions) had negligible change or remain unchanged in the presence of a single cation at  $1.0 \times 10^{-5} \text{ mol/L}$ . Thus, the sensor based on S QDs/CTSCD had good selectivity to silver ions.

### 3.6. Quenching of the S QD/CTSCD nanocomposite to silver ions.

Under optimum conditions, the sensitivity of the S QD/CTSCD nanocomposite to silver ions was investigated. In a typical operation, S QD/CTSCD solution (0.01mg/mL) was dispersed in water and mixed with different amounts of silver ions. After the samples were incubated at room temperature for 20 mins, the fluorescence emission spectra ( $\lambda_{\text{em}}=411 \text{ nm}$ ) were recorded and performed in triplicate. The fluorescence intensity was calibrated by changing the silver ions concentration.  $F_0$  and  $F$  were the

fluorescence intensities of S QDs/CTSCD in the absence and presence of silver ions at different concentrations, respectively.

Fig.7B showed that the fluorescence intensity of the S QD/CTSCD nanocomposites gradually decreased with increased concentration of silver ions because S–Ag<sup>+</sup>–S bond formed between silver ions and S QDs/CTSCD. Based on these phenomena, a favorable linear correlation ( $R^2=0.9992$ ) existed between I and silver ions concentration in the range of  $1.0 \times 10^{-5}$ – $5.5 \times 10^{-5}$  mol/L (Fig.7C), and the detection limit for silver ions was approximately 66.7 nM. The effectiveness of silver ions fluorescence detection with S QDs/CTSCD as fluorescence probe was verified and provided a platform. The selectivity of S QDs/CTSCD to silver ions might be due to the synergistic effect of S and O functional groups on S QDs/CTSCD [Lu,2014]. Where  $F_0$  ( $F_0$  was  $[C]=0$ ),  $F$  was the fluorescence intensity before and after adding silver ions,  $K_{SV}$  was the quenching effect coefficient of the sensing material,  $[C]$  was the molar concentration of the analyte (C). This quenching effect could be rationalized by the Stern–Volmer equation:  $I_0/I=1+0.0029C$  ( $R^2=0.9966$ ). The concentration of silver ions was in the range of  $1.0 \times 10^{-5}$  –  $5.5 \times 10^{-5}$  mol/L (Fig.7D). The results also showed that the S QD/ CTSCD nanocomposite was a more sensitive silver ions fluorescence sensor than others [Gao, 2020; Dager, 2019; Jiang, 2015; Lu,2014; Yang, 2020 ]. The sensitivity of the sensor was higher than that of other methods reported in literature [Lv, 2014; Gao, 2015; Wang, 2007;Bian, 2017]. As shown in Table1, the detection limit and the analytical concentration range of different technologies. Furthermore, it could be used to directly detect silver ions in the actual sample.

### 3.7 Sensor mechanism

The structure of S QDs/CTSCD should have a molecular-recognition capability to detect a certain type of substrate and provided the necessary spatial-structure arrangement for binding sites and functional groups. The functionalization of S QDs by the CTSCD structure was determined by the ability of a receptor with a heteroatom (S from S QDs, N from NH<sub>2</sub>) with lone pairs to bind silver ions. The hydration radius of silver ions could exactly match the distance on the S QDs/CTSCD nanocomposites. S QDs functionalized by the crosslinking CTSCD supramolecular structures as a component of self-assembly structure was promising because their structure contains potential coordination centers of metal cations (bridged sulfur atoms and negative charge NH<sub>2</sub> groups). The bridged S QDs in polymer structure formed S–Ag<sup>+</sup>–S bonds, which combined with colloidal particles with noncovalent bonds, thereby forming the dendritic fractal structure of aggregates based on silver ions. The experimental results showed that ACQ has occurred.

### 3.8 Effect of coexisting metal ions

To further investigate the selectivity of S QDs/CTSCD nanocomposites to silver ions, the competitive experiments were carried out by measuring the fluorescence intensity of S QDs/CTSCD nanocomposites in the presence of silver ions and additional metal ions. The effect of some co-existing cations on the detection of silver ions was shown in Figure 8. Fig.8 (B) showed the fluorescence response of the sensing

system to silver ions in the presence of other metal ions. The emission peak at 411 nm was almost no changed of most coexisting metal ions except  $\text{Ni}^{2+}$ . It could be concluded that most coexisting metal ions did not interfere with the binding of the silver ions to the S QD/CTSCD nanocomposites except  $\text{Ni}^{2+}$  ions that had a weak effect on detection. Therefore, the selective binding of silver ions could be carried out in the presence of most competitive and coexisting metal ions.

### **3.9. Detecting silver ions in environmental sample**

Environmental sample from the Xianyang Lake, Gudu Canal, and Nanhu Lake was collected. The standard  $\text{Ag}^+$  solution was added to the water samples and analyzed via standard addition method. The results showed that the recovery of silver ions in the samples were 98.44-110.76% (Table 2). The results showed that the designed sensor was reliable and practical for detecting silver ions in different environmental water samples.

## **4. Conclusion**

A convenient and green strategy of S QD/CTSCD nanocomposites was developed via simple self-assembly, which included a prior crosslinking experiment of CS and  $\beta$ -cyclodextrin. The advantages of the method lied in the aspects as follows. (1) S QDs were successfully linked to the CTSCD polymer chain through a simple and convenient self-assembly reaction and exhibited excellent fluorescence behavior. (2) S QDs/CTSCD showed a selective and sensitive response to silver ions. (3) A simple and direct method of silver ions detection was realized with fast response, wide linear range, and low detection limit. (4) Distilled water, tap water, and water from the Xianyang Lake, Nanhu Canal, and Gudu Canal were analyzed. The experimental results showed that the detection of silver ions was achieved in actual water samples. In brief, the S QDs/CTSCD nanocomposites provides new opportunities within the personal healthcare and environmental monitoring domains.

## **Declarations**

### **Data Availability Statement**

The data that support the findings of this study are available from the corresponding author upon reasonable request.

### **Authorship contribution statement**

Shan Wang: Investigation, Methodology, Writing - original draft. Yi Huang: Data curation. Yi Lu: Editing. Tian Jia and Chenyun Cai: Experiments.

### **Declaration of Competing Interest**

The authors declare that they have no known competing financial interests or personal relationships that could have appeared to influence the work reported in this paper.

## Acknowledgment:

This work was supported by National Natural Science Foundation of China (No.21703189), Xianyang Normal University “blue talent project” (XSYQL201709), Xianyang Normal University innovative project (XSYHGKZ1705). Xianyang science and technology bureau project (2019K02-27).

**Availability of data and material (Mandatory)** The data sets supporting the results of this article are included within the article and its additional files.

**Competing interests (Mandatory)** The authors declare that they have no competing financial interests

## Funding (Mandatory)

This work was supported by the National Natural Science Foundation of China (No.21703189), Xianyang Normal University “Blue Talent Project” (XSYQL201709). Shaanxi Provincial Science and Technology Department Project(2018JM2047).

## Authors' information (Optional)

Shan Wang : School of Chemistry and Chemical Engineering of Xianyang Normal University, Xianyang, 712000, PR China

## References

1. Barriada, J. L., Tappin, A. D., Evans, E. H., Achterberg, E.P., 2007, Dissolved silver measurements in seawater[J], Trends Anal. Chem., 26, 809-817. Doi: 10.16 /j.trac. 2007. 06. 004
2. Bian, S., Shen, C., Qian, Y., Liu, Xi., Dong, X., 2017, Facile synthesis of sulfur-doped graphene quantum dots as fluorescent sensing probes for Ag<sup>+</sup> ions detection[J], Sensor. Actuat. B, 242, 231–237. Doi: 10.1016/j.snb.2016.11.044
3. Chamsaz, M., Hossein, M., Akhondzadeh, J., 2008, Triple-phase single-drop microextraction of silver and its determination using graphite-furnace atomic-absorption spectrometry [J], J.Anal.Sci., 24, 799-801. Doi:10.2116/analsci. 24.799
4. Ding, C., Zhu, A., Tian, Y., 2014, Functional surface engineering of C-Dots for fluorescent biosensing and in vivo bioimaging[J], Acc. Chem. Res., 47, 20-30. Doi: 10.1021 /ar400023s
5. Dager, A., Uchida, T., Maekawa, T. et al. 2019, Synthesis and characterization of Mono-disperse carbon quantum dots from fennel seeds: photoluminescence analysis using machine learning [J].Sci. Rep., 9, 14004. Doi:10.1038 /s41598 -019 -50397-5
6. Djerahov L., Vasileva P., Karadjova I., Kurakalva R.M., Aradhi K.K., 2016, Chitosan film loaded with silver nanoparticles—sorber for solid phase extraction of Al(III), Cd(II), Cu(II), Co(II), Fe(III), Ni(II), Pb(II) and Zn(II) [J], Carbohydr. Polym., 147:45–5213. Doi:1016/j.carbpol. 2016. 03.080.

7. Fu, L., Wang, A., Xie, K., Zhu, J., Chen, F., Wang, H., Zhang, H, Su, W., Wang, Z., Zhou, C., Ruan, S., 2020, Electrochemical detection of silver ions by using sulfur quantum dots modified gold electrode[J], *Sensor. Actuat. B*, 304, 127390, Doi: 10.1016/j.snb.2019.127390
8. Gao, C, Liu, T, Dang, Y, et al. pH /redox responsive core cross- linked nanoparticles from thiolated carboxymethyl chitosan for in vitro release study of methotrexate [J]. *Carbohydr. Polym.*, 2014, 111: 964-970. Doi: 10.1016/j.carbpol.2014.05.012.
9. Gao, X., Lu, Y., Zhang, R., He, S., Li, L., Chen, W., 2015, One-pot synthesis of carbon nanodots for fluorescence turn-on detection of Ag<sup>+</sup> based on the Ag<sup>+</sup>-induced enhancement of fluorescence[J], *J. Mater. Chem. C*, 3, 2302-2309. Doi: 10.1039/c4tc02582b.
10. Goh, H., Nam, T. K., Singh, A., Singh, N., Jang, D. O., 2017, Dipodal colorimetric sensor for Ag<sup>+</sup> and its resultant complex for iodide sensing using a cation displacement approach in water[J]. *Tetrahedron Lett.*, 58, 1040-1045. Doi: 10.1016/j.tetlet. 2017.01.098
11. Hwang, K. S., Park, K. Y., Kim, D. B., Chang, S. K, 2017, Fluorescence sensing of Ag<sup>+</sup> ions by desulfurization of an acetylthiourea derivative of 2-(2-hydroxyphenyl) benzothiazole[J], *Dyes. Pigments.*, 147, 413-419. Doi: 10.1016/j.dyepig.2017.08.041
12. Jaiswal, A., Ghosh, S.S., Chattopadhyay, A., 2012, One step synthesis of C-dots by microwave mediated carbonization of poly (ethylene glycol) [J], *Chem. Commun.*, 48, 407-409. Doi: 10.1039/c1cc15988g
13. Jiang, X.K., Yusuke, I., Chong, W., Shofur, R., Parwas E. G., Xi, Z., Mark R. J. E., Carl, R., Simon J. T. and Takehiko, Y., 2018, A hexahomotrioxacalix [3]arene-based ditopic receptor for alkyl-ammonium ions controlled by Ag<sup>+</sup> ions[J], *Molecules*, 23, 467. Doi: 10.3390/molecules23020467
14. Jiang, Q., Wang, Z., Li, M., Song, J., Yang, Y., Xu, X., Xu, H., Wang, S., 2020, A nopinone based multifunctional probe for colorimetric detection of Cu<sup>2+</sup> and ratiometric detection of Ag<sup>+</sup> [J], *J. Photoch. Photobio.* 19 (1), 49-55. Doi: 10.1039/c9pp00297a
15. Jiang, Y., Kong, W., Shen, Y., Wang, B., 2015, Two fluorescence turn-on chemosensors based on pyrrolo [2,1-a] isoquinoline for detection of Ag<sup>+</sup> in aqueous solution[J], *Tetrahedron*, 71, 5584–5588. Doi: 10.1016/j.tet.2015.06.055.
16. Kim, S., Lee, H., Chae, J., Kim, C., 2020, A pyrene-mercapto-based probe for detecting Ag<sup>+</sup> by fluorescence turn-on[J], *Inorg. Chem. Commun.*, 118, 108044. Doi: 10.1016/j.inoche. 2020.108044
17. Li, C., Zhang, X., Zhang, W., Qin, X., Zhu, C., 2019, Carbon quantum dots derived from pure solvent tetrahydrofuran as a fluorescent probe to detect pH and silver ion[J], *Photobio.*, A., 382, 111981. Doi: 10.1016/j.jphotochem. 2019.111981
18. Lin, C.Y., Yu, C.J., Lin, Y.H., Tseng, W.L., 2010, Colorimetric sensing of silver(I) and mercury (II) ions based on an assembly of tween 20-stabilized gold nanoparticles[J], *Anal. Chem.*, 82, 6830-6837. Doi: 10.1021/ac1007909
19. Li, N., Bi, C., Zhang, X., Xu, C., Fan, C., Gao, W., Zong, Z., Zuo, S., Niu, C., Fan, Y., 2020, A bifunctional probe based on naphthalene derivative for absorbance-ratiometric detection of Ag<sup>+</sup> and fluorescence

- "turn-on" sensing of Zn<sup>2+</sup> and its practical application in water samples, walnut and living cells[J], *J.Photoch. Photobio., A.*, 390,112299,Doi:10.1016/ j. jphoto chem. 2019.112299
20. Lin, H., Dai, Q., Zheng, L., Hong, H., Deng, W., Wu, F., 2020,Radial basis function artificial neural network able to accurately predict disinfection by-product levels in tap water[J], *Chemosphere*, 248, 125999, Doi:10.1016/ j.chemosphere. 2020. 125999.
  21. Li, R., Fan,H.,Shen, L., Rao, L., Tang, J., Hu, S., Lin, H., 2020,Inkjet printing assisted fabrication of poly-phenol based coating membranes for oil /water separation [J],*Chemo-sphere*, 250, 126236.Doi: 10.1016 /j. chemosphere. 2020.126236.
  22. Lotfia, B., Aliakbar, T., Peyman A.M., Maryam, M.A., Ali, A. P., Jacques, M., Reza, Z., 2017, Multivalent calix [4]werene-based fluorescent sensor for detecting Ag<sup>+</sup> in aqueous media and physiological environment[J]. *Biosens. Bioelectron.*, 90, 290–297.Doi:10.1016/j.bios.2016.11. 065.
  23. Lotfi, B.,Tarlani, A., Moghaddam, P. A., Aghayan, M. M., Peyghan, A. A., Muzart, J.,Zadmard, R., 2017,Multivalent calix [4] arene-based fluorescent sensor for detecting silver ions in aqueous media and physiological environment[J].*Biosens Bioelectron.*, 90, 290-297. Doi: 10.1016 /j.bios. 2016. 11.065
  24. Lu,H.,Liang,F.,Gou,J.,Leng,J.,Du,S.,2014,Synergistic effect of Ag nanoparticle-decorated graphene oxide and carbon fiber on electrical actuation of polymeric shape memory nanocomposites[J],*Smart.Mater.Struct.*,23,085034.Doi:10.1088/0964-1726/23/8/ 085034
  25. Luidmila, S.,Yakimova, L.H.,Gilmanova, V. G., Evtugyn,Y. N., Osin,I., Stoikov, I., 2017, Self-assembled fractal hybrid dendrites from water-soluble anionic calix[4] werene and Ag<sup>+</sup>[J], *J. Nanopart. Res.*, 19:173.Doi:10.1007/s 11051-017-3868 -9
  26. Lv,Y., Zhu, L., Liu, H., Chen, Y. Z., Fu, H., Tian, Z., 2014, Single-fluorophore-based fluorescent probes enable dual-channel detection of Ag<sup>+</sup> and Hg<sup>2+</sup> with high selectivity and sensitivity[J], *Anal.Chim.Acta.*,839,74–82.Doi:10.1016/j.aca.2014.06. 010.
  27. Mikelova,R.,BalounJ.,Petrlova,J.,Adam,V.,Havel,L.,Petrek,J.,etal,2007,Electrochemical determination of Ag-ions in environment waters and their action on plant embryos[J], *Bioelectrochemistry*,70,508-518.Doi:10.1016/j.bio elechem.2006.12.001
  28. Nasrollahzadeh, M., Sajjadi, M., Iravani, S., Varma, R., 2021.Green-synthesized nanocatalysts and nanomaterials for water treatment: current challenges and future perspectives[J], *J. Hazard. Mater.* , 401,123401, Doi: 10.1016 / j.jhazmat. 2020.123401
  29. Park, J.H., Kumar, N., Park, D.H., Kang, M.H., Uhm, H.S., Choi, E.H., Attri, P.,Yusupov, M., Neyts,E.C.,Verlackt, C.C.W.,et al.2015,A comparative study for the inactivation of multidrug reswastance bacteria using dielectric barrierd was charge and nano-second pulsed plasma[J]. *Sci. Rep.*, 5, 13849. Doi:10.1038/srep1384
  30. Prasannan, A., Imae,T,2013,One-pot synthesis of fluorescent carbon dots from orange waste peels [J]. *Ind. Eng.Chem.Res.*, 52, 15673–15678. Doi: 10.1016/ j.matlet. 2014. 08.111.
  31. Rao, L., Tang, J., Hu, S., Shen, L., Xu, Y., Li, R. , 2020,Inkjet printing assisted electroless Ni plating to fabricate nickel coated polypropylene membrane with improved performance[J],*J Colloid. Interface.*

- Sci., 565, 546- 554. Doi: 10.1016/j. jcis. 2020. 01.069.
32. Singha, S., Kim, D., Seo, H., Cho, S. W., Ahn, K. H., 2015. Fluorescence sensing systems for gold and silver species[J], Chem. Soc. Rev., 44, 4367-4399. Doi: 10.1039/c4cs00328d
  33. Singh, S., Numan, A., Zhan, Y., Singh, V., Van H., Nam, N., 2020, A novel highly efficient and ultrasensitive electrochemical detection of toxic mercury (II) ions in canned tuna fish and tap water based on a copper metal-organic framework[J], J. Hazard. Mater., 399, 123042, Doi: 10.1016 /j.jhazmat.2020.123042
  34. Shan W., Xing B., Bei G., Meng L., 2019, A novel sulfur quantum dot for the detection of cobalt ions and norfloxacin as a fluorescent "switch" [J], Dalton Trans., 48, 8288-8296. Doi: 10.1039/c9dt01186b
  35. Spokoyny, A. M., Kim, D., Sumreinand A., Mirkin, C. A., 2009, Infinite coordination polymer nano-microparticle structures[J], Chem. Soc. Rev., 38, 1218–1227. Doi: 10.1039 / b807085g
  36. Tabaraki R., Nateghi A. Nitrogen-doped graphene quantum dots: "turn-off" fluorescent probe for detection of Ag<sup>+</sup> ions[J]. J. Fluoresc., 2016, 26(1):297-305. Doi: 10.1007 /s10895 -015 -1714-y
  37. Teng, Shen, L., Xu, Y., Chen, Y., Wu, X., He, Y., Chen, Y., 2020, Effects of molecular weight distribution of soluble microbial products (SMPs) on membrane fouling in a membrane bioreactor (MBR): novel mechanistic insights[J], Chemosphere, 248, 126013. Doi: 10.1016 /j. chemosphere.
  38. Teng, J., Wu, M., Chen, J., Lin, H., He, Y., 2020. Different fouling propensities of loosely and tightly bound extracellular polymeric substances (EPSs) and the related fouling mechanisms in a membrane bioreactor[J], Chemosphere, 255, 126953. Doi: 10.1016/ j.chemosphere.2020. 126953.
  39. Vaishnav, J.K., Mukherjee, T.K., 2019, Surfactant-induced self-assembly of CdTe quantum dots into multicolor luminescent hybrid vesicles[J], Langmuir, 35(19), 6409-6420. Doi: 10.1021 / acs. langmuir. 9b00357
  40. Velmurugan, K., Raman, A., Easwaramoorthi, S., Nandhakumar, R., 2014, Pyrene pyridine -conjugate as Ag<sup>+</sup> selective fluorescent chemosensor [J], RSC. Adv., 4, 35284-35289. Doi: 10.1039 /c4ra04001e.
  41. Wu, M., Chen, Y., Lin, H., Zhao, L., Shen, L., Li, R., Xu, Y., Hong, H., He, Y., 2020, Membrane fouling caused by biological foams in a submerged membrane bioreactor: mechanism insights [J], Water. Res., 181, 115932. Doi: 10.1016/j. waters. 115932.
  42. Wang, J. H., Wang, H. Q., Zhang, H. L., Li, X. Q., Hua, X. F., Zhao, Y. D., 2007, Purification of denatured bovine serum albumin coated CdTe quantum dots for sensitive detection of silver(I) ions [J], Anal. Bioanal. Chem., 388, 969–974. Doi: 10.1007 /s00216-007-1277-0
  43. Xiao, Y., Cui, Y., Zheng, Q., Xiang, S., Qian, G., Chen, B., 2010, A microporous luminescent metal –organic framework for highly selective and sensitive sensing of Cu<sup>2+</sup> in aqueous solution[J]. Chem. Commun., 46, 5503–5505. Doi: 10.1039/c0c c00148a
  44. Yang, Y., Liu, Y., Chen, S., Cheong K., Teng, B., 2020, Carboxymethyl-cyclodextrin grafted carboxymethyl chitosan hydrogel-based microparticles for oral insulin-delivery, Carbohydr. Polym., Doi: 10.1016/ j.carbpol.2020.116617.

45. Zhang, C., Hu, M., Ke, Q., Guo, C., Guo, Y., Guo, Y., 2020, Nacre-inspired hydroxylapatite / chitosan layered composites effectively remove lead ions in continuous- flow wastewater[J], J. Hazard. Mater., 386,121999, Doi: 10.1016 / j.jhazmat.2019.121999
46. Zhang, Y., Ye, A., Yao, Y., Yao, C., 2019, A sensitive near-infrared fluorescent probe for detecting heavy metal Ag<sup>+</sup> in water samples[J], Sensors, 19(2), 247/1 -247/12. Doi: 10.3390 / s19020247
47. Zheng, M., Xie, Qu,Z., Li, D., Du, P., Jing, X., et al, 2013,On-off-on fluorescent carbon dot nanosensor for recognition of chromium(VI) and ascorbic acid based on the inner filter effect[J], ACS Appl. Mater. Interfaces, 5, 13242-13247. Doi: 1021 /am 4042355

## Tables

Due to technical limitations, table 1,2 is only available as a download in the Supplemental Files section.

## Figures

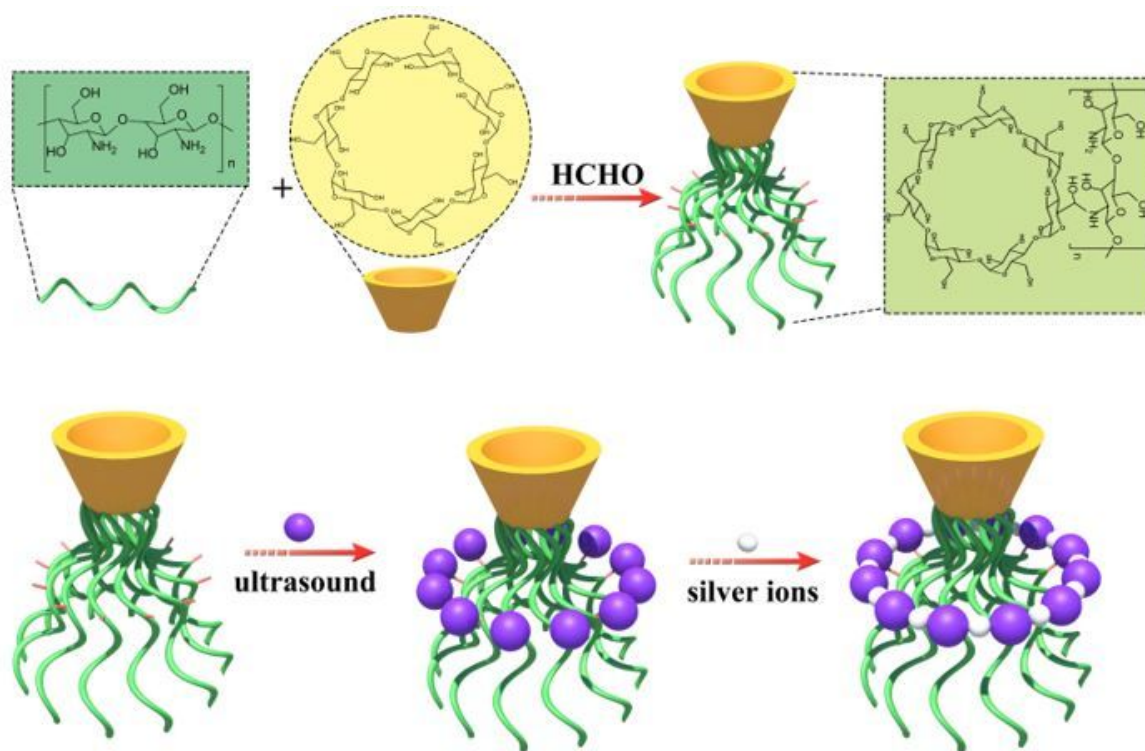
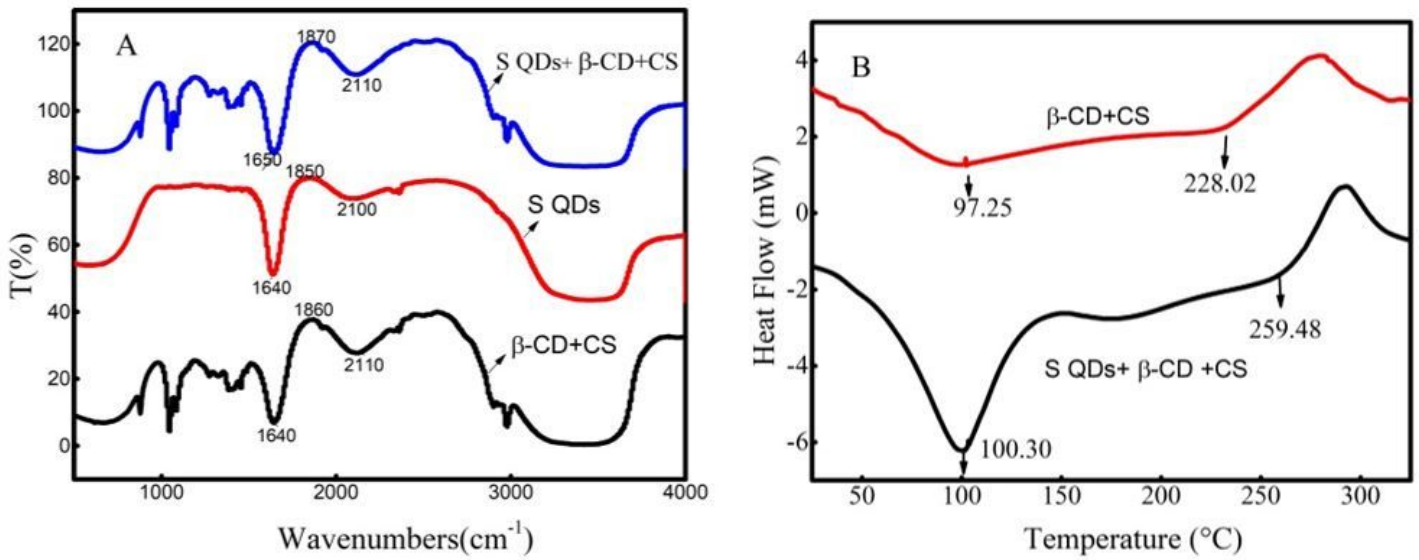


Figure 1

The possible mechanism of the novel sensor



**Figure 2**

The FTIR (A) and DSC (B) of the S QDs/CTSCD nanocomposites

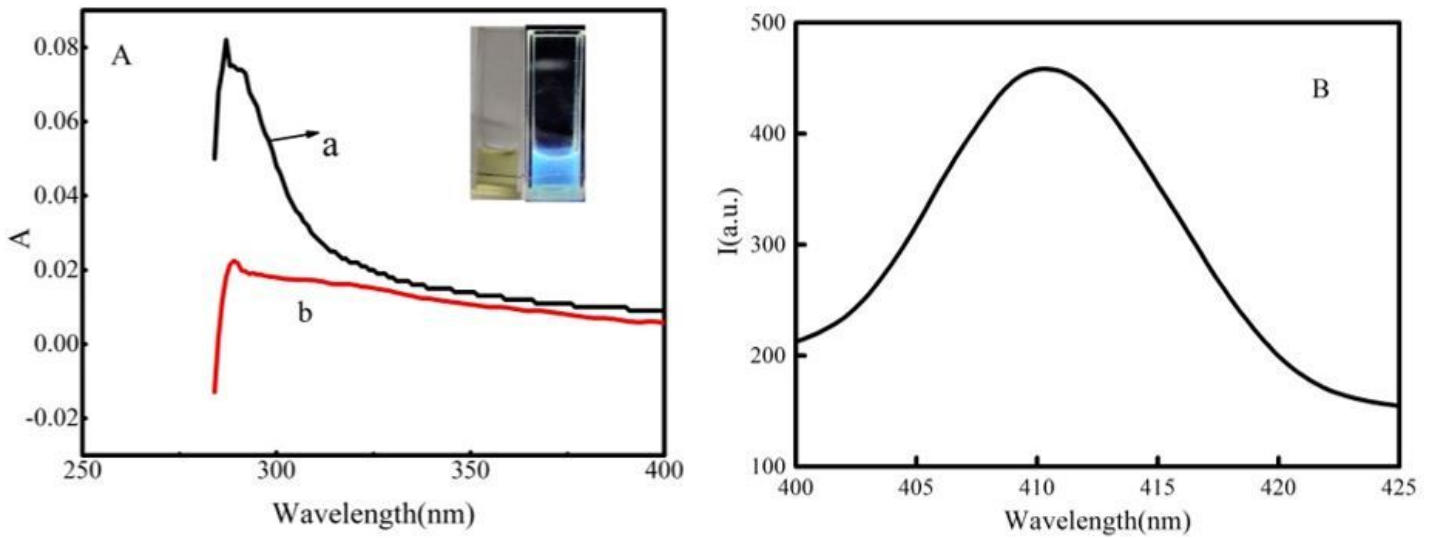


**Figure 3**

The UV/Vis spectra (A) and maximum fluorescence emission (B) of the S QDs/CTSCD nanocomposites

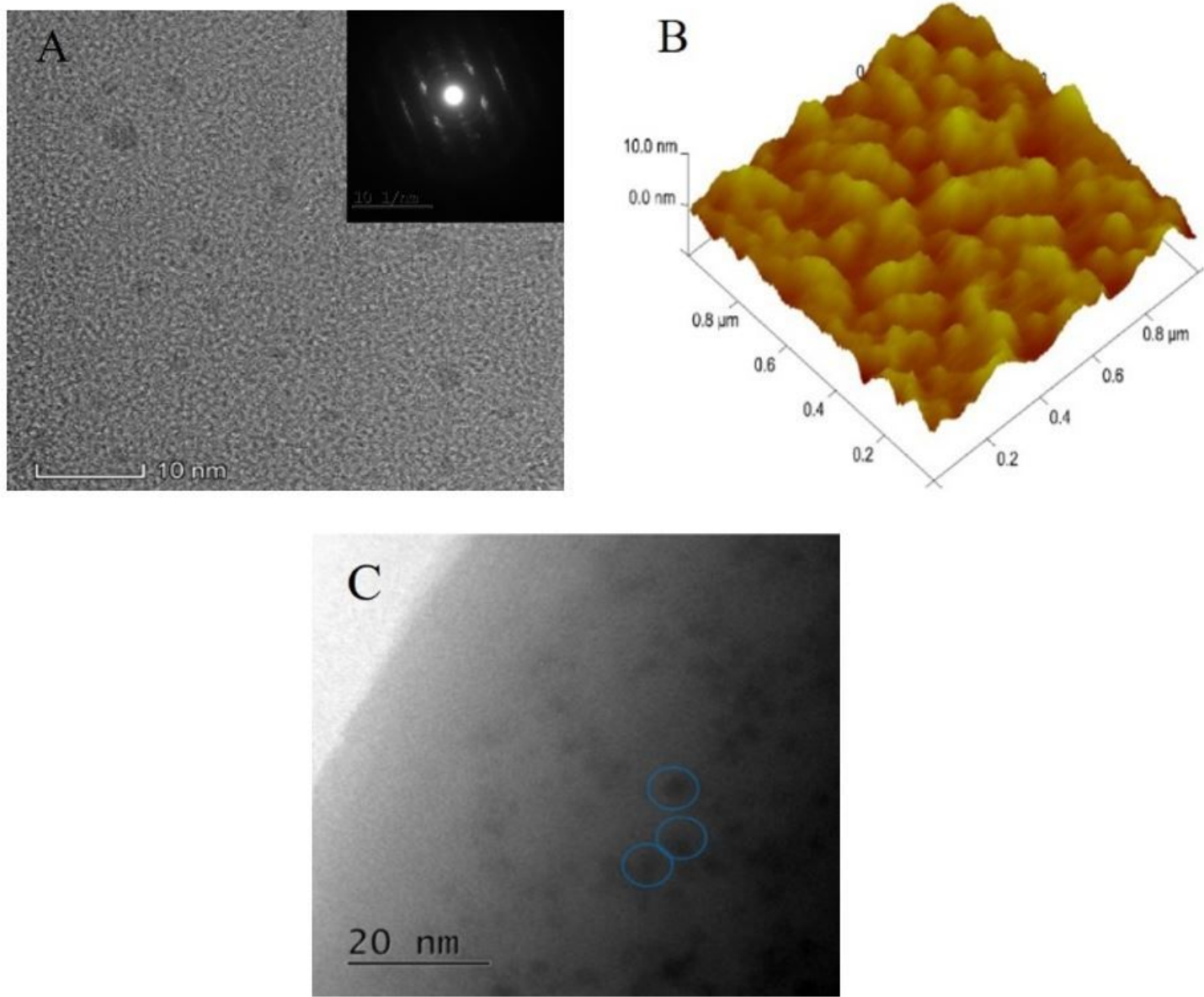


**Figure 4**

(A) TEM image of S QDs with diameter around 2-3 nm; (B) AFM representation of S QDs; and (C) The TEM of the S QDs/CTSCD nanocomposites.

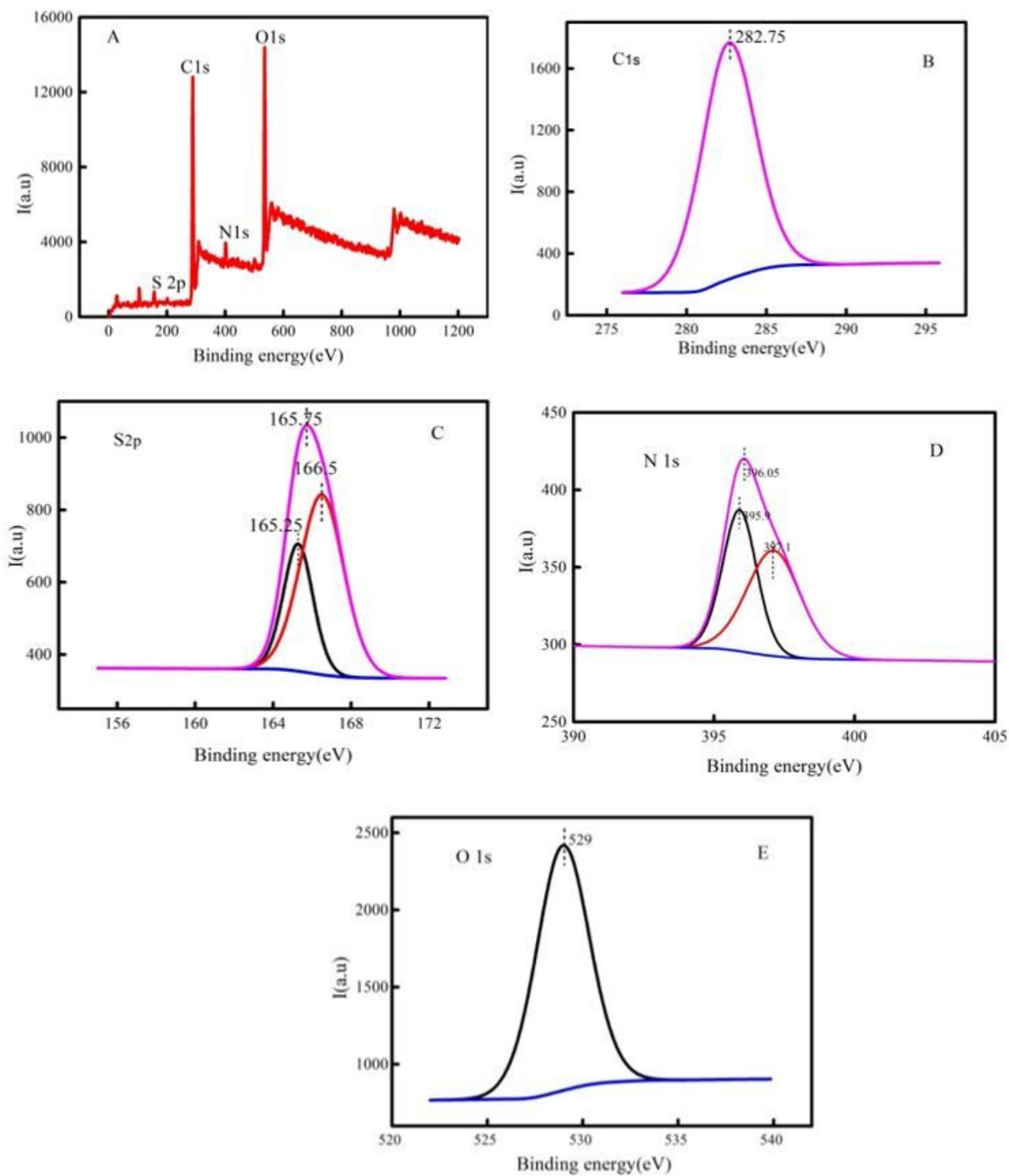


**Figure 5**

The XPS characterization of S QDs/CTSCD nanocomposites

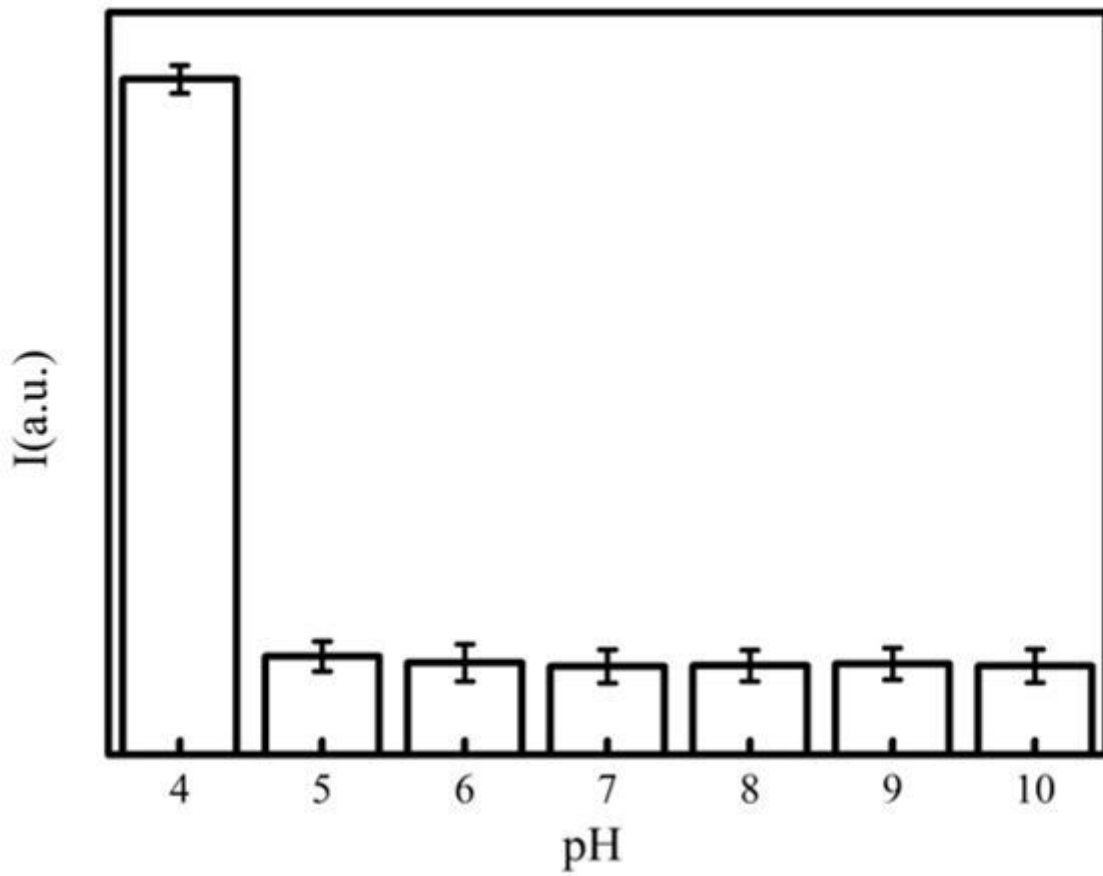


**Figure 6**

Effect of pH on the fluorescence properties of S QDs/ CTSCD nanocomposites

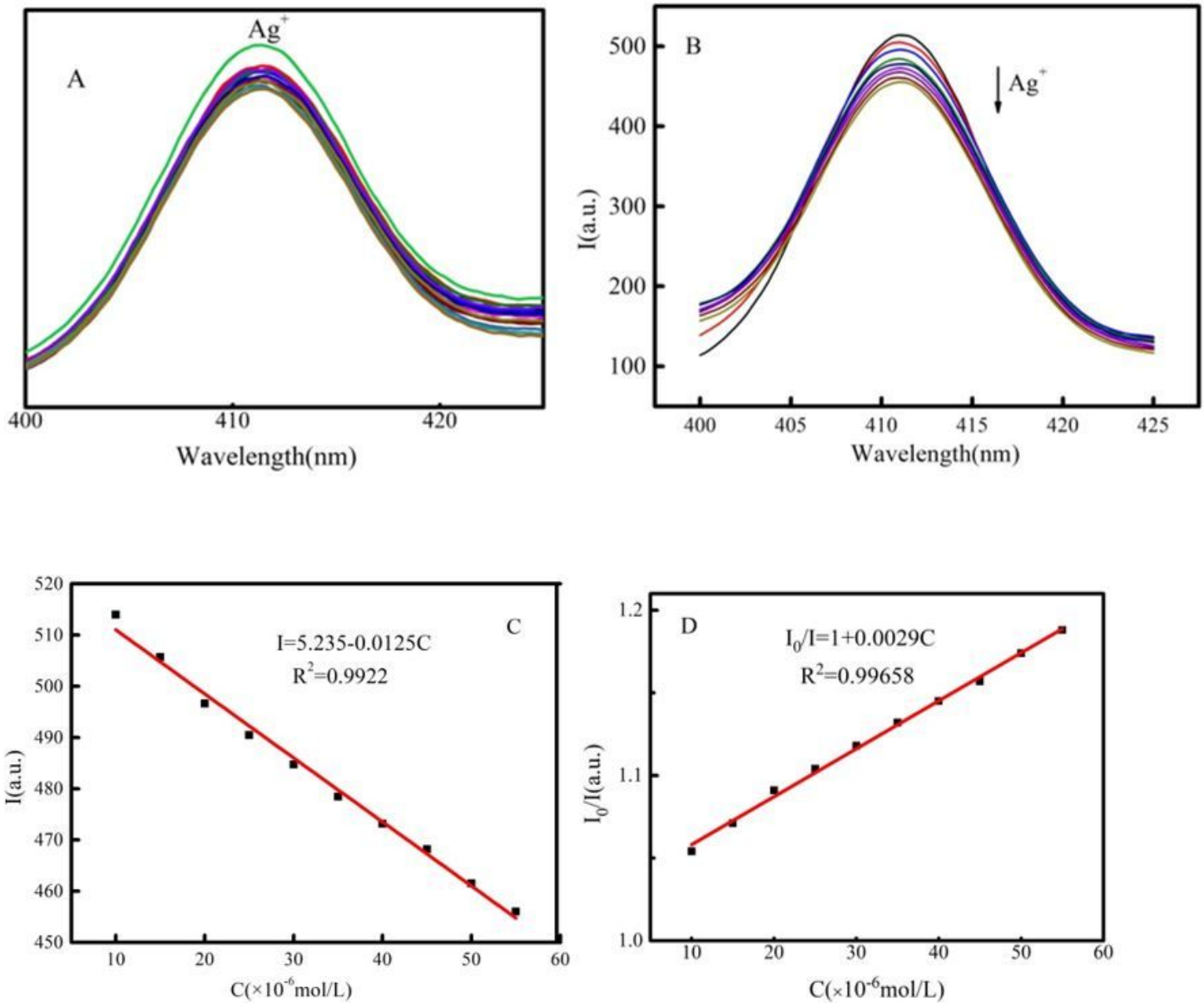


**Figure 7**

Study on the sensing properties of S QDs/CTSCD nanocomposites (A, Selectivity B, Sensing properties (Silver ion concentration from  $1 \times 10^{-5}$  mol/L to  $5.5 \times 10^{-5}$  mol/L), C, Linear properties D, S-V equation) C  $Ag^+$ : 1,  $1 \times 10^{-5}$  mol/L; 2,  $1.5 \times 10^{-5}$  mol/L; 3,  $2 \times 10^{-5}$  mol/L; 4,  $2.5 \times 10^{-5}$  mol/L; 5,  $3 \times 10^{-5}$  mol/L; 6,  $3.5 \times 10^{-5}$  mol/L; 7,  $4 \times 10^{-5}$  mol/L; 8,  $4.5 \times 10^{-5}$  mol/L; 9,  $5 \times 10^{-5}$  mol/L; 10,  $5.5 \times 10^{-5}$  mol/L)

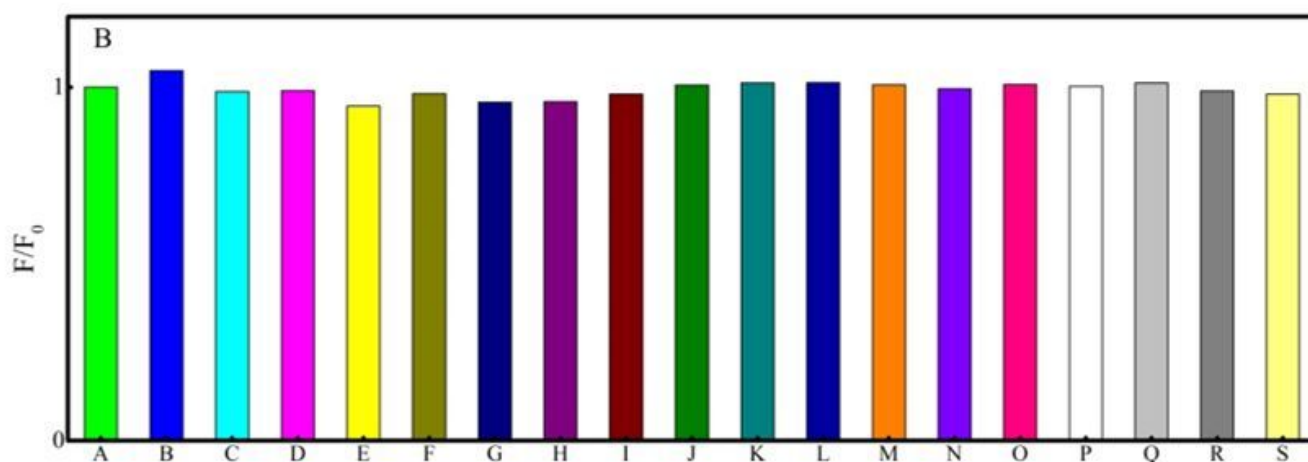
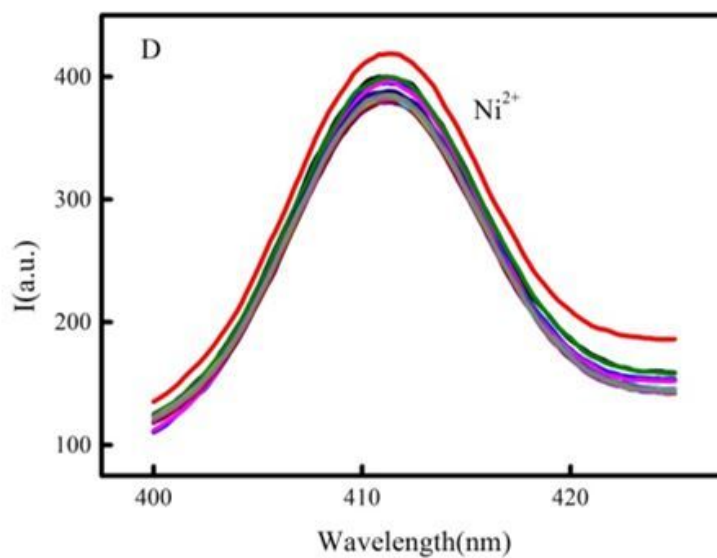


**Figure 8**

Interference of different inorganic metal ions in the sensing of silver ions by S QDs/CTSCD nanocomposites (A: Ag<sup>+</sup>, B: Ni<sup>2+</sup>, C: Mn<sup>2+</sup>, D: Fe<sup>2+</sup>, E: Mo<sup>6+</sup>, F: Cu<sup>2+</sup>, G: Fe<sup>3+</sup>, H: Ca<sup>2+</sup>, I: Pb<sup>2+</sup>, J: Na<sup>+</sup>, K: Cr<sup>3+</sup>, L: Bi<sup>3+</sup>, M: Zn<sup>2+</sup>, N: Mg<sup>2+</sup>, O: Ba<sup>2+</sup>, P: Cd<sup>2+</sup>, Q: Sr<sup>2+</sup>, R: Hg<sup>2+</sup>, S: Co<sup>2+</sup>)

## Supplementary Files

This is a list of supplementary files associated with this preprint. Click to download.

- [Graph.docx](#)
- [Table1.jpg](#)

- [Table2.jpg](#)